

Article

# A Novel Thermostable Cytochrome P450 from Sequence-Based Metagenomics of Binh Chau Hot Spring as a Promising Catalyst for Testosterone Conversion

Kim-Thoa Nguyen <sup>1,2,\*</sup>, Ngọc-Lan Nguyen <sup>2,3</sup>, Nguyen Van Tung <sup>2,3</sup>, Huy Hoang Nguyen <sup>2,3</sup> , Mohammed Milhim <sup>4</sup>, Thi-Thanh-Xuan Le <sup>1</sup>, Thi-Hong-Nhung Lai <sup>1</sup>, Thi-Tuyet-Minh Phan <sup>1</sup> and Rita Bernhardt <sup>4</sup> 

<sup>1</sup> Institute of Biotechnology, Vietnam Academy of Science and Technology (VAST), 18 Hoang Quoc Viet, Cau Giay, Hanoi 100000, Vietnam; xuankhanhan@gmail.com (T.-T.-X.L.); hanhunglai@gmail.com (T.-H.-N.L.); phanthituyetminh1973@gmail.com (T.-T.-M.P.)

<sup>2</sup> Graduate University of Science and Technology, Vietnam Academy of Science and Technology (VAST), 18 Hoang Quoc Viet, Cau Giay, Hanoi 100000, Vietnam; lannguyen@igr.ac.vn (N.-L.N.); tungnv53@gmail.com (N.V.T.); nhhoang@igr.ac.vn (H.H.N.)

<sup>3</sup> Institute of Genome Research, Vietnam Academy of Science and Technology (VAST), 18 Hoang Quoc Viet, Cau Giay, Hanoi 100000, Vietnam

<sup>4</sup> Department of Biochemistry, Saarland University, 66123 Saarbrücken, Germany; abomajid13@hotmail.com (M.M.); ritabern@mx.uni-saarland.de (R.B.)

\* Correspondence: nkthoa@ibt.ac.vn; Tel.: +84-24-37567103

Received: 17 August 2020; Accepted: 16 September 2020; Published: 18 September 2020



**Abstract:** Biotechnological applications of cytochromes P450 show difficulties, such as low activity, thermal and/or solvent instability, narrow substrate specificity and redox partner dependence. In an attempt to overcome these limitations, an exploitation of novel thermophilic P450 enzymes from nature via uncultured approaches is desirable due to their great advantages that can resolve nearly all mentioned impediments. From the metagenomics library of the Binh Chau hot spring, an open reading frame (ORF) encoding a thermostable cytochrome P450—designated as P450-T3—which shared 66.6% amino acid sequence identity with CYP109C2 of *Sorangium cellulosum* So ce56 was selected for further identification and characterization. The ORF was synthesized artificially and heterologously expressed in *Escherichia coli* C43(DE3) using the pET17b system. The purified enzyme had a molecular weight of approximately 43 kDa. The melting temperature of the purified enzyme was 76.2 °C and its apparent half-life at 60 °C was 38.7 min. Redox partner screening revealed that P450-T3 was reduced well by the mammalian AdR-Adx<sub>4-108</sub> and the yeast Arh1-Etp1 redox partners. Lauric acid, palmitic acid, embelin, retinoic acid (*all-trans*) and retinoic acid (*13-cis*) demonstrated binding to P450-T3. Interestingly, P450-T3 also bound and converted testosterone. Overall, P450-T3 might become a good candidate for biocatalytic applications on a larger scale.

**Keywords:** thermostable P450; CYP109C; metagenomic; P450-T3; fatty acids; testosterone; biocatalyst; redox partner; expression; half-life; melting temperature; Binh Chau hot spring

## 1. Introduction

Cytochromes P450 (CYPs) belong to one of the largest enzyme superfamilies, which is widely distributed in all living organisms like bacteria, fungi, plants and animals [1,2]. They play a crucial role in life by catalyzing more than 20 types of reactions in regio- and stereoselective manners, such as hydroxylation, dealkylation, epoxidation, oxidation, dehalogenation, dehydrogenation and

reduction. To carry out these functions, their substrates are also diversified, varying from drugs and xenobiotics to complex substances, this way taking part in the metabolism of drugs, the biosynthesis and metabolism of endogenous compounds and the biosynthesis of valuable substances [3]. Bacterial P450s play an important role in xenobiotic bioremediation as well as in the diversification of natural products due to their capacity to oxidatively degrade the natural substances and artificial chemicals through hydroxylation or epoxidation and to perform the above mentioned reactions on natural molecules [4]. Many reactions are difficult to perform chemically on a pilot and/or industrial scales, especially when producing medical substances. One of the criteria for enzymes deployed on an industrial scale is durability, including thermal stability [5]. However, the instability of P450s under industrial production conditions, such as high temperatures and large amounts of organic solvents limited their applications for large-scale production [6,7]. Consequently, seeking thermostable P450s from nature has attracted attention. Thermostable P450s can be used in the production of valuable organic compounds [8]. Furthermore, using thermostable P450s also has the advantage of building a two-phase production system. Substrates of heat resistant P450 (usually organic compounds in nature) can interact with enzymes in the solvent phase to be converted into diffusion products in the water phase. The first known thermostable P450 (CYP119) was found in the archaea *Sulfolobus solfataricus* [9]. Initial characterization revealed that this enzyme had a melting temperature of approximately 90 °C, which was determined by the differential scanning calorimetry method with a scan rate of 70 °C/h over the temperature range 25–100 °C [10]. This melting temperature was considerably higher than that of mesophilic P450s. CYP119 was capable of catalyzing the epoxidation of styrene and cis-stilbene as well as the hydroxylation of fatty acids [11,12]. CYP175A1 of *Thermus thermophilus* HB27 was the second heat resistant P450 described and recognized as the first P450 capable of hydroxylation of  $\beta$ -carotene [13]. The melting temperature of CYP175A1 was 88 °C, while that of mesophilic P450s ranged from 47–61 °C [14].

To date, a limited small number of thermostable P450 have been reported and they mainly belong to several thermophiles, such as CYP119A1, CYP119A2, CYP174A1, CYP175A1, CYP231A2, CYP154H1 and several members of the CYP116B subfamily (CYP116B29, CYP116B46, CYP116B63, CYP116B64, and CYP116B65) [15,16]. Furthermore, bacterial CYP102A2 and the human CYP2B subfamily and CYP3 family were rationally or/and semi-rationally designed for greater thermostability [15–17].

Numerous microbial thermostable P450s still exist in nature and have not been exploited, especially from nonculturable extremophilic microorganisms, where the enzyme cannot be acquired from a conventional culture of the microorganisms. The Japanese Institute of Marine Biotechnology has developed a “cassette PCR” method for sequencing genes coding for enzymes producing target biological compounds. This method allows for obtaining a target DNA fragment from metagenomic analysis of the environment and designates a gene that encodes the marker protein for active screening. Kubota et al. [18] applied this method to acquire 16 new cytochrome P450 *CYP153A* genes from a variety of environmental sources, such as oil-contaminated soil, groundwater, and n-alkane-degrading bacterium *Alcanivorax borkumensis* SK2. The discovery of P450s from new sources or new species continues to attract the exploration of metagenomic DNA. Kim et al. [19] discovered a gene that encodes for a new self-sufficient P450, called *syk181*, from the metagenomic library of soil collected from the Keryong Mountain, South Korea. The SYK181 shared a 46% amino acid sequence identity to CYP102A1. Furthermore, CYP102A1 was only capable of metabolizing fatty acids, whereas SYK181 was able to metabolize both fatty acids and aromatic compounds, such as naphthalene and phenanthrene. These positive results inspired us to look for thermostable P450s in geothermal natural sources, such as hot springs, oil-drilling, and volcanoes, by metagenomics approaches. Hot springs are suitable habitats of thermophiles and extremophiles which have optimum growth temperatures above 55 °C and 80 °C, respectively. Many enzymes exploited from those sources have been demonstrated to be extremely useful for industrial and biotechnological purposes [20].

Vietnam is endowed with a diverse geothermal system with more than three hundred hot springs scattered from the North to the South. The Binh Chau hot spring (10°36'05.0'' N and 107°33'33.5'' E)

located in the Ba Ria province and is the second hottest hot spring in Vietnam. The average opened mouth temperature is 80 °C, hence, this location is a potential resource for finding thermophiles and thermostable enzymes. The sequencing and analysis of 9.4 Gb DNA metagenomics from the Binh Chau hot spring by Illumina HiSeq Platform revealed the presence of 68 putative ORFs encoding for putative monooxygenase enzymes, which belong to 36 different P450 subfamilies [21]. Based on the melting temperature index program (<http://tm.life.nthu.edu.tw/>), a novel sequence, soluble P450-T3, was selected due to its predicted melting temperature of >65 °C. Subsequently, its cDNA was synthesized and expressed, and the protein was purified for characterization. The purified recombinant enzyme showed thermal stability, coupled with several artificial electron transfers and bound a broad spectrum of substrates.

## 2. Results

### 2.1. Identification and Bioinformatic Analyses of P450-T3

P450-T3 shared the highest sequence identity (69%) with cytochrome P450 CYP109C2 of *Sorangium cellulosum* So ce56 at the amino acid level. P450-T3 also showed 66.6% identity with CYP109C2 from *S. cellulosum* So ce56 according to Dr. Nelson's Cytochrome P450 Homepage (<https://drnelson.uthsc.edu/CytochromeP450.html>).

The phylogenetic tree obtained with MEGA X revealed that P450-T3 formed a cluster with other members of the CYP109C subfamily, which were identified in *S. cellulosum* (Supplementary Figure S1), suggesting that P450-T3 belongs to the CYP109C subfamily.

Multiple amino acid sequence alignments of P450-T3 with its closest homologs reveal the presence of the three conserved domains of cytochrome P450 (Figure 1). The oxygen binding and activation motif AGXTT is located in I-helix (residues 222–227) [22], of which the highly conserved threonine probably plays an important role in catalysis [23]. The EXXR motif (residues 261–264) contains the conserved glutamic acid and arginine in all the cytochromes P450 that build a set of salt-bridge interactions to form the final P450 tertiary structure [24]. The heme-binding domain motif FXXGXXCXCXG (residues 325–334) contains the three most conserved residues in the cytochrome P450 superfamily, including phenylalanine, glycine, and cysteine, of which the conserved cysteine plays the role of the axial ligand to the heme [25].

### 2.2. Production and Purification of P450-T3

For expression purpose, the *P450-T3* gene was successfully cloned into the pET17b vector and expressed in the *Escherichia coli* C43(DE3) strain. The carbon monoxide (CO) difference spectrum was recorded according to the Omura and Sato methods [26]. The results showed a typical peak with a maximum at 450 nm without another peak at 420 nm (Figure 2a), indicating that the protein was produced in an active conformation. The yield of recombinant P450-T3 was 585 nmol/L bacterial cell culture before purification. The purified enzyme was shown to have a molecular weight of approximately 43 kDa on SDS-PAGE as predicted (inset of Figure 2a). UV-Vis spectroscopy revealed that P450-T3 contains a heme molecule as a prosthetic group, which is involved in the generation of the Soret ( $\gamma$ ) band at 418 nm (Figure 2b), and the smaller  $\alpha$  and  $\beta$  bands at 567.5 and 536 nm, respectively (inset of Figure 2b), indicating a low-spin state of heme iron.

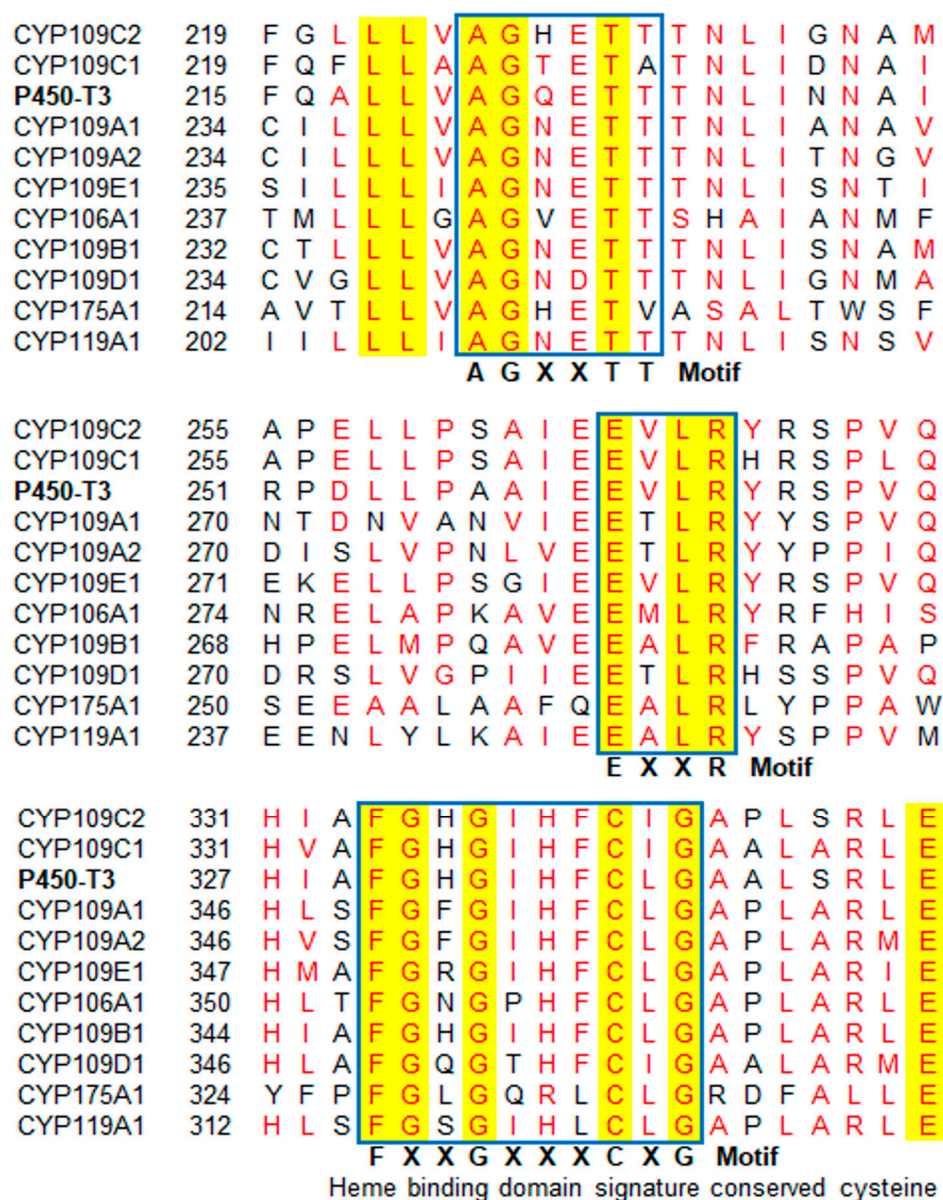


**Figure 1.** Sequence alignment of P450-T3 with members of the CYP109 family and other known thermostable enzymes. Conserved and similar residues are highlighted in red font and yellow background, respectively. Blue frames show the AGXXTT and EXXR motifs and heme-binding domain signature FXXGXXXCXG.

The secondary structure of an enzyme can be identified rapidly by using circular dichroism (CD) spectroscopy. The CD spectra were recorded in the far-UV and near UV visible region. The far-UV CD spectrum showed double bands with minima at 211 and 222 nm (Figure 2c), a representation of combined contribution of helical and  $\beta$ -strand structures [27]. P450-T3 was predicted to consist of 64.16% regular secondary elements (53.77% the  $\alpha$ -helix and 10.39% strand of  $\beta$ -sheet) and 35.84% coil as an irregular secondary element (Supplementary Figure S2). In the near UV-visible region, P450-T3 displayed two large negative signals at 350 nm and at 408 nm (Figure 2d). These are in correspondence with the characteristic peaks for other bacterial P450s [28,29].

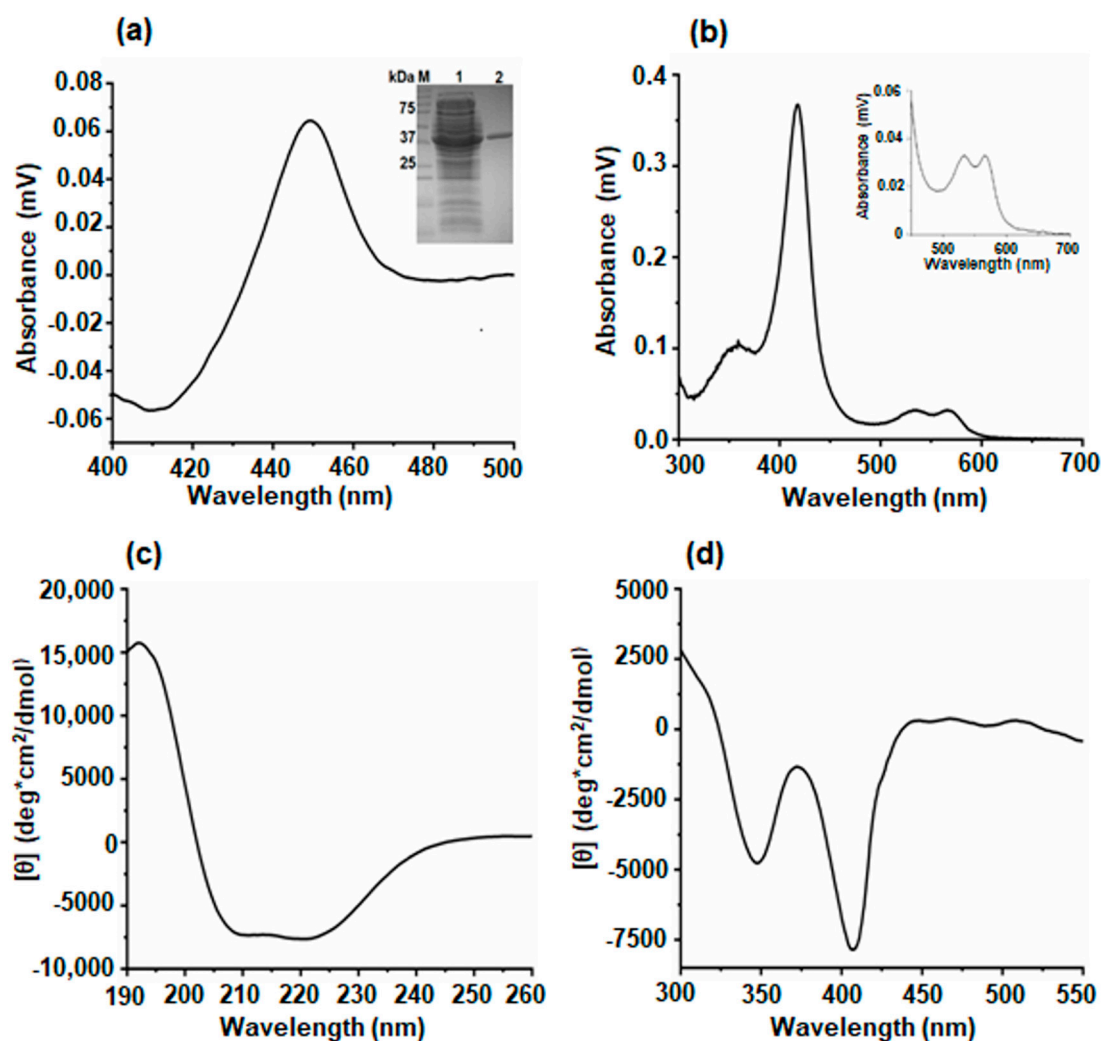


**Figure 2.** Spectroscopic characterization of P450-T3. (a) The typical carbon monoxide (CO) difference spectrum of P450-T3. In the inset, SDS-PAGE of the expression and purification of P450-T3. Lane 1: Precision protein marker (Biorad). Lane 2: Cell lysate after 48 h of expression. Lane 3: purified P450-T3. (b) The UV-Vis spectral analysis of the purified P450-T3. The magnification of the spectrum in the  $\alpha$  and  $\beta$  band region was shown in the inset. The molar ellipticity was converted based on the circular dichroism (CD) spectra in the far-UV (c) and in the near UV-Vis region (d).

### 2.3. Thermal Stability of P450-T3

The effect of temperature on P450-T3 structural integrity was investigated using various spectral methods. P450-T3 showed the highest integrity at 50–60 °C and lost it at 70 °C (Figure 3a). The far-UV CD spectra were recorded between 190–260 nm every 10 °C to determine the changes in their secondary structure as a function of the temperature [30]. In the inset of Figure 3b, the appearance of an intense negative minimum around 208 and 222 nm and a positive maximum around 197 nm confirmed the existence of a predominant  $\alpha$ -helical secondary structure [27]. The presence of an isodichroic point at 203 nm (inset of Figure 3b) indicated a dominant  $\alpha$  to  $\beta$  structural thermal transition. The thermal stability curve of P450-T3 was evaluated by recording the increment in the CD signal at a 211 nm wavelength over the temperature range from 25–95 °C. At 70 °C, a little loss of magnitude of the negative CD signal was observed, compared to those at temperatures of 30–60 °C. It means that, at a temperature of  $\geq 70$  °C, P450-T3 lost helical secondary structure. This phenomenon was clearly observed at 80 °C and 90 °C. The overlap of CD signals of protein P450-T3 at temperatures  $\leq 60$  °C suggested that the helical secondary structure of P450-T3 was stable at 60 °C. Moreover, in the thermal

stability curve determined by CD (Figure 3b), we observed that P450-T3 started to change the helical structure at 67 °C. A rapid inactivation was shown after incubation at 80 °C. The calculated  $T_m$  was  $76.2 \pm 0.05$  ( $R^2 = 0.99$ ).

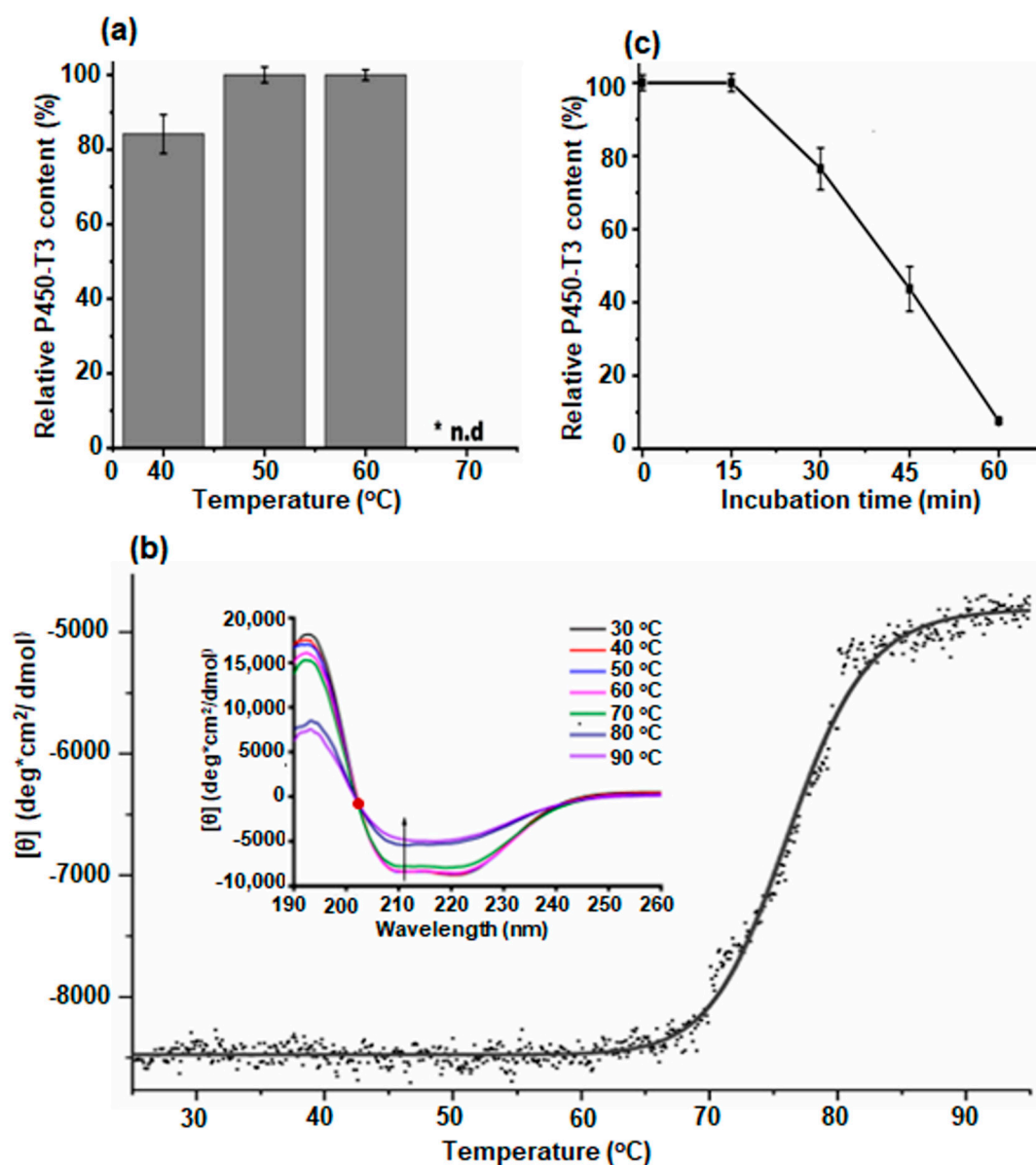


**Figure 3.** Thermal stability of P450-T3. (a) The optimal temperature of P450-T3 was evaluated through CO difference spectroscopy after incubating the enzyme at 40, 50, 60 and 70 °C. (b) Melting curve of P450-T3 recorded by circular dichroism (CD). The temperature slope of 1 °C per min with a resolution of 0.1 °C was used to determine the ellipticity at 211 nm as a function of temperature in the range between 25–95 °C. The inset shows far-UV CD spectra of P450-T3 at the indicated temperatures. Red circle indicates the isodichroic point. Arrows show the direction of the peak by increasing the temperature at 211 nm. The CD spectra were recorded between 190–260 nm every 10 °C and converted into molar ellipticity units. (c) The  $T_{1/2}$  of P450-T3 was identified at 60 °C from 0–60 min where the P450 content was measured every 15 min.

Measuring the half-life ( $T_{1/2}$ ) at optimal temperature is another parameter for evaluating thermal stability. The  $T_{1/2}$  of P450-T3 was determined by incubating the enzyme at 60 °C and measured by CO difference spectroscopy every 15 min to calculate the relative stability (Figure 3c). The  $T_{1/2}$  of P450-T3 was 38.7 min at 60 °C.

#### 2.4. Identification of Electron Transfer Partners

Cytochromes P450s are heme-containing monooxygenases which require a coupled and stepwise supply of electrons to start oxidation and hydroxylation reactions [3]. For efficient catalysis, P450s require an electron transfer chain (in bacteria mostly a ferredoxin reductase and ferredoxin). In nature, microorganisms can use autologous electron transfer partners. In this study, under laboratory conditions, we tested the compatibility of P450-T3 with known ferredoxin reductase/ferredoxin partners, including BmCPR-Fdx2, BmCPR-Fdx3, Arh1-Etp1 and AdR-Adx<sub>4-108</sub>. The diflavin reductase BmCPR and ferredoxin Fdx2 are electron transfer partners of *Bacillus megaterium* DSM319. The BmCPR-Fdx2 system efficiently supported the activity of CYP106A1 [31] and CYP107DY1 [32]. The bovine adrenodoxin reductase homologue 1 Arh1 and its natural redox partner Etp1 are originated from *Schizosaccharomyces pombe* [33]. The Arh1/Etp1 system was demonstrated to be efficient for a biotechnological application with CYP105A1 from *Streptomyces griseolus* [34,35]. The bovine adrenodoxin reductase (AdR) and adrenodoxin (Adx<sub>4-108</sub>) were identified as the most efficient redox partners for several myxobacteria cytochrome P450s [36,37].

The redox partners were compared on the base of the spectra of the reduced CO-complexed enzyme of P450-T3 (Figure 4). The redox partners BmCPR-Fdx3 did not produce a significant Soret peak at 450 nm. The redox partners BmCPR-Fdx2 reduced by ~15% in the CO complex sample. The systems AdR-Adx<sub>4-108</sub> and Arh1-Etp1 showed a higher efficiency with ~30% of peak recovered (compared to dithionite). The redox system AdR-Adx<sub>4-108</sub> was selected for further investigation of P450-T3.

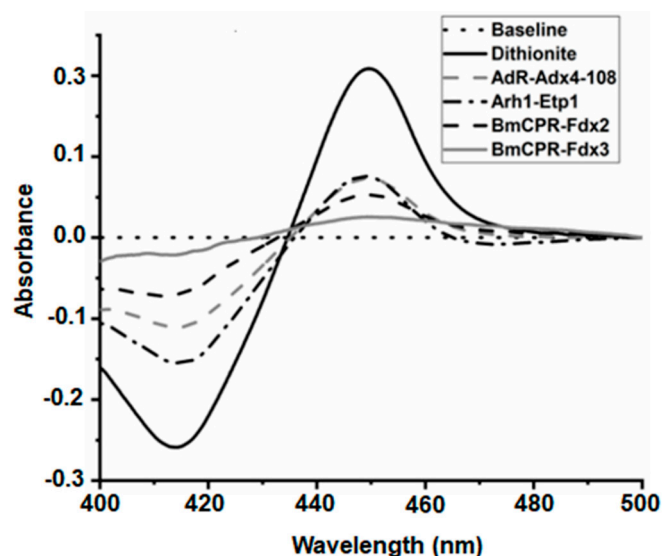


**Figure 4.** Screening of electron transfer partners for P450-T3. The dithionite reduced CO-difference spectrum (black solid line) was compared with the CO-complex spectrum after reduction by AdR-Adx<sub>4-108</sub> (gray dash line), Arh1-Etp1 (black dash-dot line), BmCPR-Fdx2 (black dash line), and BmCPR-Fdx3 (gray solid line). The baseline is shown as a dotted line. A 1 mL mixture of P450-T3:ferredoxin:ferredoxin reductase (1:40:5) dissolved in 50 mM HEPES buffer (pH 7.4). NADPH solution (1 mM) was supplemented for starting the reduction.

#### 2.5. Substrate Screening for P450-T3

Seeking for the substrate specificity of an individual cytochrome, P450, especially of a novel enzyme, is a significant effort that helps to expand its potential application. Since P450-T3 was identified as a close relative of CYP109C2 from *S. cellulosum* So ce56—which is a fatty acid hydroxylase [38], lauric acid, palmitic acid—and other substances sharing a structural part of fatty acids, such as retinoic acid (*all-trans*), and retinoic acid (*13-cis*) and embelin were used to evaluate their ability to bind to P450-T3. The results showed a transition from low-spin state to high-spin state of the heme pocket

for all the substances used (Table 1), indicating a broader potential substrate spectrum for P450-T3 in comparison with CYP109C2.

**Table 1.** Substrate binding of P450-T3.

Compound	Shift from Low-Spin to High-Spin
Lauric acid	+
Palmitic acid	+
Embelin	+
Retinoic acid ( <i>all-trans</i> )	+
Retinoic acid ( <i>13-cis</i> )	+
11-Deoxycorticosterone (DOC)	-
11-Deoxycortisol (RSS)	-
Progesterone	-
Testosterone	+
Nootkatone	-

+ indicates binding and - indicates no binding of the substrate to the P450-T3 was detected.

Enzyme members of the CYP109 subfamilies have different substrate specificities. For example, CYP109A2 from *B. megaterium* DSM319 was involved in vitamin D3 hydroxylation [39], whereas CYP109D1 from *S. cellulosum* So ce56 was demonstrated to oxidize norisoprenoids [40]. CYP109E1 from *B. megaterium* DSM319 [41] and CYP109B1 from *B. subtilis* W23 [42] showed the capacity of steroid conversions. Besides steroid conversion, CYP109B1 was reported to hydroxylate  $\alpha$ - and  $\beta$ -ionone [43]. To date, CYP109E1 has shown the broadest substrate spectrum, being involved not only in steroid conversion, but also in the hydroxylation of vitamin D3, vitamin D2, cholesterol, statins, and terpenes [39,41,44,45]. Therefore, P450-T3 might also exhibit novel characteristics, including an altered substrate specificity. In this study, nootkatone and several steroids, such as 11-deoxycorticosterone (DOC), 11-deoxycortisol (RSS), progesterone, and testosterone were tested. Interestingly, testosterone was observed to bind to P450-T3 (Table 1). It was further investigated in in vitro conversion assays. Using the redox system AdR-Adx<sub>4-108</sub> for in vitro reconstitution, P450-T3 showed the ability to convert testosterone into two products at a retention times of 13.5 and 15 min, respectively (Figure 5). The conversion ratio of 100  $\mu$ M testosterone was  $\sim$  11% in total after 30 min.

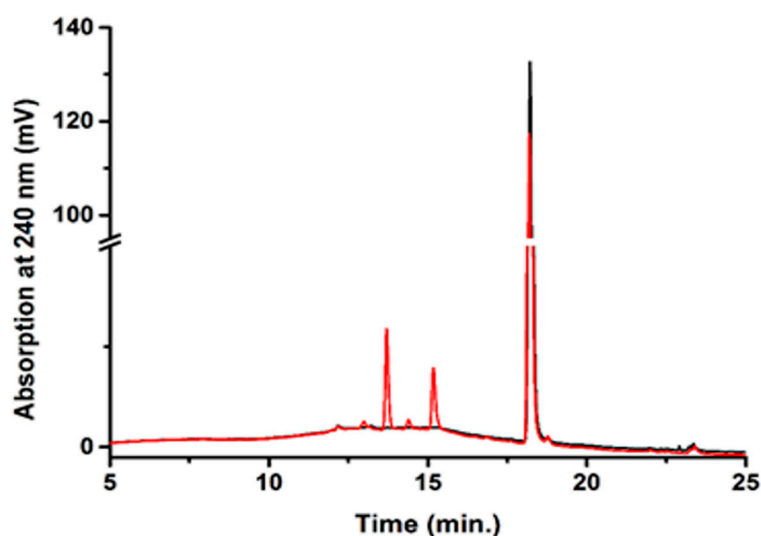


**Figure 5.** HPLC analysis of the in vitro conversion of testosterone with P450-T3. The reaction was carried out in 50 mM HEPES buffer (pH 7.4) with 20% glycerol. The black line indicates negative control (testosterone without P450-T3) and the red line represents for testosterone converted by P450-T3 for 30 min at 37 °C.

### 3. Discussion

Recently, considerable attention has been paid towards identification and characterization of new thermostable P450s due to their potential use in industrial processes. Until now, only few thermostable P450s were found from thermophilic microorganisms in nature, including CYP119 from *S. solfataricus* [46], CYP119A1 from *T. thermophilus* [14], CYP119A2 from *S. tokodaii* [47], CYP175A1 from *T. thermophilus* [13], CYP154H1 from *Thermobifida fusca* [48], CYP231A2 from *P. torridus* [49], and CYP116B subfamilies from several archaea species [15,16]. However, the number of thermostable cytochrome P450s is still insufficient for versatile biocatalysis on a larger scale. To enhance the catalytic efficiency, different strategies have been used, such as the engineering of proteins, redox-partner interactions, substrates, and electron sources [50], of which the improvement in cytochrome P450s is the main effort and challenge. Besides the molecular evolution of these enzymes, another approach—metagenomics—was introduced in 2004 by Handelsman et al. [51]. Until now, metagenomics is a well-accepted power tool for exploiting the microbial genome in a natural environment. Several enzymes have been successfully discovered using this method, such as hydrolases [52–56], oxidoreductases [57], dehydratases [58], and cytochrome P450s (e.g., CYP153A members) [18]. Recently, 264 putative CYP153 proteins were identified from the metagenomic dataset obtained from 23 sediment samples [59]. Their characteristics were computed to point out a highly promising application for catalysis using a broad variety of substrates under cold conditions. The advantage of using metagenomics is especially visible in extreme habitats, such as geothermal ecologies (volcanoes, hot spring) and offshore oil platform. Most of the thermostable enzymes have been produced by thermophilic microorganisms in hot springs or through metagenomic analysis of this environment [60–62]. Vietnam has a diverse hot spring system which allows us to find desired enzymes. To the best of our knowledge, this is one of the first examples of identifying thermostable cytochrome P450s that rely on metagenome-based sequences in the Binh Chau hot spring. Here, we report on the characterization of one of them, P450-T3. Bioinformatic analyses of the amino acid sequence of P450-T3 indicated that it shares the highest identity with CYP109C2 of *S. cellulosum* So ce56. However, P450-T3 does not belong to the CYP109C2 subfamily due to a moderate bootstrap value. This finding might indicate a novel CYP109C subfamily, which is one of the smallest families among bacterial P450s with so far only eight subfamily members (<https://cyped.biocatnet.de/sFam/109>). Moreover, analyses of 16S rRNA database in the metagenomics of the Binh Chau hot spring revealed that *S. cellulosum* accounts for ~0.00438% (data not shown). Therefore, it was supposed that P450-T3 might have originated from this myxobacterial species.

As compared to other thermostable cytochrome P450s, P450-T3 showed an optimal temperature of 60 °C, which is lower than that of CYP119A1 from *S. solfataricus* (70 °C [9]), but higher than that of CYP154H1 from *T. fusca* (50–55 °C [48]). The melting temperature of P450-T3 was calculated to be 76.2 °C, which was higher than that of CYP154H1 (67 °C [48]) and CYP231A2 (65 °C [49]), but lower than those of CYP119A1 (90 °C [9]) and CYP175A1 (87 °C [13]). The thermal stability of a protein was ascribed to a variety of global aspects, as described by Yano et al. [14], Zhou et al. [63], and Lee et al. [64]. In comparison with the mesophilic P450BM-3, the thermostable P450-T3 shows an increase in alanine (11.7% versus 9.1%) and arginine residues (8.6% versus 4.2%) and a decrease in lysine (2.3% versus 6.7%) and glutamine residues (4.4% versus 5.2%). Alanine is the best-helix-forming residue [65]; therefore, a higher alanine content in the  $\alpha$ -helix (16.43% versus 12.15%) in P450-T3 may make the protein more thermal stability. The reduction in glutamine in P450-T3 is consistent with the findings of several studies [66,67], in which the composition of uncharged polar residues (glutamine, threonine, serine) is much lower in thermophiles than those in mesophiles.

On the other hand, the half-life ( $T_{1/2}$ ) of an enzyme is an important index to evaluate its stability. Protein engineering has a great impact on enzyme stability. CYP102A1 from *B. megaterium* was engineered to strengthen the thermal stability of the reductase domain, which led to an increase in the optimal temperature from 25 to 40 °C and prolonged its half-life at 50 °C ten-fold [68]. Moreover, Urlacher et al. [69] created a library of chimeric fusion proteins by exchanging the unstable reductase

domain of CYP102A1 with the more stable reductase domain of CYP102A3, resulting in a chimeric protein displaying a wider temperature range and broader substrate specificity. The  $T_{1/2}$  of the new chimeric protein at 50 °C was 100 min, which was more than ten-fold longer than that of the wild type. P450-T3 displayed a  $T_{1/2}$  at 60 °C of 37.5 min, which is a moderate thermostability as compared to other CYPs. However, as described for CYP102A1, it might be further increased by using protein engineering techniques, such as site-directed mutagenesis or directed evolution.

P450-T3 is an external monooxygenase. Therefore, it requires an external electron donor in the electron transfer chain to transfer electrons from NADPH to its heme for substrate hydroxylation. In this study, the used redox pairs BmCPR-Fdx2 and BmCPR-Fdx3, originating from *B. megaterium*, were not or only partly able to interact with P450-T3. Similar to CYP109C1 and CYP109C2 from *S. cellulosum* So ce56, P450-T3 accepted the reduction equivalents from bovine AdR- Adx<sub>4-108</sub> and yeast Arh1-Etp1 [38]. However, the reduction yield of P450-T3 was low, (Figure 5). Hence, a suitable ratio between P450-T3 and the redox partner may be identified in the future to optimize the electron transfer.

The next important question was to identify possible substrates for P450-T3. The similarity to CYP109C1 and CYP109C2 from *S. cellulosum* So ce56 indicated the ability to bind to medium-chain fatty acid (lauric acid) and unsaturated long-chain fatty acids (e.g., palmitic acid). As shown in Table 1, the substrate spectrum binding to P450-T3 is more diverse than that of the thermostable CYP175A1, which only showed the ability to bind to some unsaturated monoenoic fatty acids but not to saturated fatty acids [70]. It has to be demonstrated in future studies whether the bound substrates can also be converted by P450-T3, since this not always the case [71]. Lauric acid and palmitic acid are the main fatty acids in coconut oil and palm kernel oil; therefore, P450-T3 might be used in oil production in the future. Moreover, long aliphatic chain (embelin) and tretinoin (retinoic acid (*all-trans*), as well as retinoic acid (*13-cis*)), also bind as potential substrates to P450-T3, suggesting that P450-T3 may be used for the production of biopharmaceuticals. Embelin and its derivatives are used in cancer treatments and display other biological activities [72]. Retinoic acid (*all-trans*) and retinoic acid (*13-cis*) are two main substances used in dermatology for acne as well as steroid-damaged skin treatment, despite of some negative effects [73–75]. It will, therefore, be of high interest to investigate their conversion by P450-T3 and to identify the formed products.

Since steroids are broadly marketed drugs, together with antibiotics and antibodies, their derivatives have attracted much attention. Steroid hydroxylation results in hydroxylated products with high level of biological activity [76]. Interestingly, P450-T3 was able to convert testosterone into two products. However, under the conditions used here, the ratio of conversion only reached ~ 11% in total. A variety of factors may affect testosterone conversion, such as an insufficient redox partner, improper temperature, and/or the inappropriate ratio of the components in the reconstituted system. The role of P450-T3 in Binh Chau hot spring environment, as well as the sequences of putative natural reductases and ferredoxins, which can serve as redox partners of P450-T3, is still unexplored. It is thus of high interest to identify a thermostable redox partner to finally optimize the condition for substrate conversion and to be able to characterize the obtained products of substrate conversion. Despite the presently low catalytic efficiency of testosterone conversion, this is, to the best of our knowledge, the first report of testosterone conversion of a thermostable P450 and of a member of the CYP109C subfamily.

Taken together, our findings demonstrate that P450-T3 is a novel thermostable P450 with an astonishing broad ability to bind different kinds of substrate. It might be a potential biocatalyst for versatile drug production. These results also are very useful for further biochemical studies and biotechnological applications of P450-T3.

## 4. Materials and Methods

### 4.1. Materials

The 1158 bp ORF encoding for P450-T3, comprising 385 amino acids, was subjected in this study. This ORF was synthesized and ligated into *pUC19* vector by Phusa Biochem Ltd. (Cantho, Vietnam). The nucleotide and amino acid sequences of P450-T3 were deposited in the NCBI GenBank under the accession number MT232930.

The *E. coli* strain Top 10 was purchased from Invitrogen (San Diego, CA, USA). The *E. coli* strain C43(DE3) was obtained from Agilent Technologies (Santa Clara, CA, USA).

The ORF of P450-T3 was cloned into a *pET17b* plasmid (Novagen, Darmstadt, Germany) using the forward primes 5'-gatccatggtggccttggcagctcca-3' and the reverse primes 5'-gatcaagcttagtggtgatggtgatgctggccttgagctgcagca-3' that contained *NdeI* and *HindIII* restriction sites (underline), respectively. These primers were synthesized by MWG Biotech AG (Ebersberg, Germany).

Embelin, retinoic acid (*all-trans*), retinoic acid (*13-cis*) were kindly provided by Dr. Stephan Lütz (Novartis, Basel, Switzerland). A couple of redox partner enzymes, such as the mammalian AdR-Adx<sub>4-108</sub>, the yeast Arh1-Etp1, and the *Bacillus* systems (BmCPR-Fdx2, BmCPR-Fdx3), were supported by the Department of Biochemistry, University of Saarland (Saarbrücken, Germany). All other chemicals and reagents were of the highest grade available.

### 4.2. Methods

#### 4.2.1. Bioinformatics Analysis

The DNA sequence was translated using the ExPaSy Translate tool (<https://www.expasy.org/>). Identification of close homologs was performed using the Basic Local Alignment Search Tool (BLAST, NCBI) and Dr. Nelson's Cytochrome P450 Homepage [77]. Alignment of multiple amino acid sequences was performed with Clustal Omega [78]. Evolutionary analyses were conducted in MEGA X [79]. The evolutionary history was inferred with the maximum likelihood approach and Le\_Gascuel model [80]. The content of secondary elements of proteins was calculated using PRIPRED tool [81].

#### 4.2.2. Production and Purification of P450-T3

The ORF P450-T3 was amplified using the pair of primers described above and cloned into the *pET17b* vector (Novagen, Darmstadt, Germany) with the *NdeI/HindIII* restriction sites. The clones (pET-T3) were checked with both restriction enzymes before sequencing by MWG Biotech AG (Ebersberg, Germany).

The vector pET-T3 was transformed into *E. coli* C43(DE3), competent cells for heterologous gene expression. The main culture was inoculated at 37 °C in 250 mL Terrific Broth (TB) medium containing 100 µg/mL ampicillin to achieve an OD<sub>600</sub> of 0.8–1. Protein production was induced by adding 1 mM isopropyl-β-D-thiogalactopyranoside (IPTG) and 0.5 mM δ-aminolevulinic acid as a precursor for heme synthesis. The cells were harvested after 48 h expression at 30 °C and shaken at 150 rpm.

The cell pellets were resuspended and sonicated in 50 mL lysis buffer (50 mM potassium phosphate buffer, pH 7.4, containing 20% glycerol, 0.1 mM dithioerythritol, 500 mM sodium acetate, and 1 mM phenylmethanesulfonyl fluoride) [32]. The lysate was centrifuged at 35,000 rpm and 4 °C for 30 min. Cell debris was removed and the supernatant was loaded onto a Ni-NTA agarose column equilibrated with lysis buffer. After washing with 100 mL of the equilibration buffer containing a gradient of 20–50 mM imidazole, protein was eluted with 20 mL elution buffer (50 mM potassium phosphate, pH 7.4, containing 1% Tween 20, 10% glycerol, 0.1 mM dithioerythritol, 0.1 mM phenylmethanesulfonyl fluoride, and 200 mM imidazole). Fractions with A<sub>417</sub>:A<sub>280</sub> >1.6 were collected and dialyzed overnight to remove imidazole. The protein was concentrated by Centriprep (Millipore, MA, USA) with a pore size of 50 kDa and 30 kDa to the expected volume before storing at –80 °C.

The concentration of P450 enzyme was estimated by CO difference spectroscopy assuming  $\Delta\epsilon_{(450-490)} = 91 \text{ mM}^{-1} \cdot \text{cm}^{-1}$  as described by Omura and Sato [26]. UV-visible spectra for the purified P450 enzyme was recorded at room temperature from 200 to 700 nm on a double-beam spectrophotometer (UV2101PC, Shimadzu, Kyoto, Japan).

#### 4.2.3. Circular Dichroism Spectroscopy

The far-UV CD spectra (195–260 nm) and the near-UV spectra (300–450 nm) were recorded with 4 and 20  $\mu\text{M}$  purified P450-T3, respectively, in 10 mM potassium phosphate buffer pH 7.4 at 25 °C on a JASCO J715 spectropolarimeter, as described by Khatri et al. [38]. Molar ellipticity  $[\theta]$  was calculated in  $\text{deg} \cdot \text{cm}^2/\text{dmol}$  using the following equation:

$$[\theta] = m^\circ \cdot M / (10 \cdot L \cdot C) \quad (1)$$

where  $m^\circ$  is the CD millidegree,  $M$  is the average molecular weight of P450-T3 (g/mol),  $L$  is path length of cell (cm), and  $C$  is concentration of sample.

#### 4.2.4. Thermal Stability

The optimal temperature of P450-T3 was identified by CO difference spectroscopy. Enzyme samples (10  $\mu\text{M}$ ) were incubated for 15 min at 40, 50, 60, and 70 °C, respectively, and the retained amount of the active form of P450 (absorption in the CO spectrum at 450 nm) was estimated.

The enzyme melting curve was evaluated from its far-UV CD spectrum as an important measure of thermal stability. The purified protein was dissolved in 20 mM of mM potassium phosphate buffer pH 7.4 to obtain a concentration of 20  $\mu\text{M}$ . The enzyme was scanned using a Chirascan CD spectrometer between 190–260 nm while recording every 1 nm for 0.5 s per nm with a bandwidth of 5 nm. Each spectrum was acquired independently three times. Then, the melting curve was obtained by monitoring the CD at 211 nm over a temperature range 25–95 °C at a rate of 1 °C per min. At each temperature, the enzyme was able to equilibrate for 30 s before recording the CD. Melting temperature was obtained from the second-derivative plots of the melting curve.

Another parameter related to enzyme stability is the enzyme half-life inactivation ( $T_{1/2}$ ). To determine  $T_{1/2}$ , the purified P450-T3 was dissolved in 20 mM potassium phosphate buffer, pH 7, and incubated at 60 °C. Samples were taken every 15 min, and the residual absorption at 450 nm in the CO difference spectrum was measured. The  $T_{1/2}$  index was calculated by the following equation:

$$T_{1/2} = \ln 2 / K_d \quad (2)$$

where  $K_d$  is the first-order rate constants determined by linear regression of  $\ln$  (residual absorption at 450 nm) versus the incubation time ( $t$ ) [82,83].

#### 4.2.5. Investigation of Electron Transfer Partners

The functional interaction of the electron transfer partners for a P450-T3 was examined by recording the NADPH reduced CO-complex peak at 450 nm when P450-T3 was combined with the different ferredoxins (Fdx2/Fdx3/Adx<sub>4-108</sub> or Etp1)/ferredoxin reductase (BmCPR, AdR or Arh1) pairs in the absence of substrate, as described by Milmim et al. [32].

#### 4.2.6. Monitoring of Substrate Binding

The substrate binding of the enzyme was followed by a transition of Soret bands from low-spin state which shows a maximal peak at 417 nm to high-spin state where the maximal peak raised at around 390 nm. The measurement was carried out by adding substrates in the excess ratio of 1:15 or 1:20 and monitored in the range of 200–700 nm at room temperature on a double-beam spectrophotometer (UV2101PC, Shimadzu, Kyoto, Japan). The kind of substrates varied from fatty acids (palmitic acid

and lauric acid) to metabolites (embelin, retinoic acid (*all-trans*) and retinoic acid (*13-cis*)) and steroids (11-deoxycorticosterone (DOC), 11-deoxycortisol (RSS), progesterone, and testosterone).

#### 4.2.7. In Vitro Conversion of Testosterone and HPLC Analysis

A reconstituted in vitro system was used in a final volume of 250  $\mu\text{L}$  at 37 °C in a buffer (50 mM HEPES, pH 7.4, and 20% glycerol) which consisted of 1  $\mu\text{M}$  P450-T3, 2.5  $\mu\text{M}$  AdR, 20  $\mu\text{M}$  Adx<sub>4-108</sub>, 1 mM MgCl<sub>2</sub>, 5 mM glucose-6-phosphate, 1 U glucose-6-phosphate dehydrogenase, and 100  $\mu\text{M}$  testosterone. The addition of 200  $\mu\text{M}$  NADPH started the conversion. After 30 min, the conversion was stopped by adding ethyl acetate (250  $\mu\text{L}$ ) and extracted twice. The negative control was carried out parallel in the absence of enzyme to verify the P450-dependent reaction. The organic phase was evaporated before resolving the precipitate by acetonitrile for HPLC analysis.

HPLC analyses were performed on the Jasco system (Gross-Umstadt, Germany) consisting of a Pu-980 HPLC pump, an AS-950 sampler, a UV-975 UV/visible detector, and an LG-980-02 gradient unit. Steroids and their metabolites were observed by a UV-Vis detector at 240 nm and 25 °C when crossing the Macherey–Nagel CC125/4 Nucleodur C<sub>18</sub>ec column (3  $\mu\text{m}$ , 125  $\times$  4.0 mm, Macherey–Nagel, Düren, NRW, Germany) with gradient elution from 10% to 100% acetonitrile over 30 min.

## 5. Conclusions

In this study, a novel thermostable cytochrome P450-T3 from the Binh Chau hot spring metagenomics database was identified, synthesized, expressed, and characterized. The enzyme had a higher optimal temperature (60 °C) compared to mesophilic cytochrome P450s with a melting temperature at 76.2 °C. P450-T3 exhibited a broad substrate binding ability, including lauric acid, palmitic acid, embelin, retinoic acid (*all trans*), retinoic acids (*13-cis*), and testosterone. We further identified heterologous redox partners for this P450 and investigated the conversion of testosterone, which was shown to be converted by P450-T3 into two products. Our results contribute to the database of natural thermostable cytochrome P450s, which is still limited so far. Furthermore, the enzyme toolbox can be expanded with thermostable P450s via an uncultured approach, which is useful for biotechnological applications in the future.

**Supplementary Materials:** The following are available online at <http://www.mdpi.com/2073-4344/10/9/1083/s1>, Figure S1: Phylogenetic tree of P450-T3 in the cluster of the CYP109 family. Evolutionary analyses were conducted in MEGA X. Figure S2: Prediction of secondary structures of P450-T3 using the PRIPRED tool.

**Author Contributions:** Conceptualization, K.-T.N. and R.B.; methodology, M.M. and H.H.N.; software, N.V.T.; validation, N.-L.N.; investigation, K.-T.N., T.-T.-X.L., T.-H.-N.L. and T.-T.-M.P.; resources, K.-T.N. and H.H.N.; data curation, N.V.T. and M.M.; writing—original draft preparation, K.-T.N. and N.-L.N.; writing—review and editing, K.-T.N. and R.B.; visualization, N.-L.N. and M.M.; supervision, K.-T.N.; project administration, K.-T.N. All authors have read and agreed to the published version of the manuscript.

**Funding:** This research is funded by Vietnam National Foundation for Science and Technology Development (NAFOSTED) under grant number 106-NN.02-2014.60.

**Acknowledgments:** Special thanks are sent to Ngo Ba Huong in Saigon Binh Chau Corporation for supporting us to get the hot spring samples.

**Conflicts of Interest:** The authors all declare no conflict of interest. The funders had no role in the design of the study; in the collection, analyses, or interpretation of data; in the writing of the manuscript, or in the decision to publish the results

## References

1. Werck-Reichhart, D.; Feyereisen, R. Cytochromes P450: A success story. *Genome Biol.* **2000**, *1*, reviews3003.1. [[CrossRef](#)] [[PubMed](#)]
2. Nelson, D.R. Cytochrome P450 diversity in the tree of life. *Biochim. Biophys. Acta* **2018**, *1866*, 141–154. [[CrossRef](#)] [[PubMed](#)]
3. Bernhardt, R. Cytochromes P450 as versatile biocatalysts. *J. Biotechnol.* **2006**, *124*, 128–145. [[CrossRef](#)] [[PubMed](#)]

4. Urlacher, V.; Schmid, R.D. Biotransformations using prokaryotic P450 monooxygenases. *Curr. Opin. Biotechnol.* **2002**, *13*, 557–564. [[CrossRef](#)]
5. Niehaus, F.; Bertoldo, C.; Kähler, M.; Antranikian, G. Extremophiles as a source of novel enzymes for industrial application. *Appl. Microbiol. Biotechnol.* **1999**, *51*, 711–729. [[CrossRef](#)]
6. O'Reilly, E.; Köhler, V.; Flitsch, S.L.; Turner, N.J. Cytochromes P450 as useful biocatalysts: Addressing the limitations. *Chem. Commun.* **2011**, *47*, 2490–2501. [[CrossRef](#)]
7. Bernhardt, R.; Urlacher, V.B. Cytochromes P450 as promising catalysts for biotechnological application: Chances and limitations. *Appl. Microbiol. Biotechnol.* **2014**, *98*, 6185–6203. [[CrossRef](#)]
8. Syed, K.; Shale, K.; Nazir, K.H.M.N.H.; Krasevec, N.; Mashele, S.S.; Pagadala, N.S. Genome-wide identification, annotation and characterization of novel thermostable cytochrome P450 monooxygenases from the thermophilic biomass-degrading fungi *Thielavia terrestris* and *Myceliophthora thermophila*. *Genes Genom.* **2014**, *36*, 321–333. [[CrossRef](#)]
9. Wright, R.L.; Harris, K.; Solow, B.; White, R.H.; Kennelly, P.J. Cloning of a potential cytochrome P450 from the archaeon *Sulfolobus solfataricus*. *FEBS Lett.* **1996**, *384*, 235–239. [[CrossRef](#)]
10. McLean, M.A.; Maves, S.A.; Weiss, K.E.; Krepich, S.; Sligar, S.G. Characterization of a Cytochrome P450 from the Acidothermophilic Archaea *Sulfolobus solfataricus*. *Biochem. Biophys. Res. Commun.* **1998**, *252*, 166–172. [[CrossRef](#)]
11. Koo, L.S.; Tschirret-Guth, R.A.; Straub, W.E.; Moënnel-Locoz, P.; Loehr, T.M.; Ortiz de Montellano, P.R. The active site of the thermophilic CYP119 from *Sulfolobus solfataricus*. *J. Biol. Chem.* **2000**, *275*, 14112–14123. [[CrossRef](#)]
12. Koo, L.S.; Immoos, C.E.; Cohen, M.S.; Farmer, P.J.; Ortiz de Montellano, P.R. Enhanced electron transfer and lauric acid hydroxylation by site-directed mutagenesis of CYP119. *J. Am. Chem. Soc.* **2002**, *124*, 5684–5691. [[CrossRef](#)] [[PubMed](#)]
13. Blasco, F.; Kauffmann, I.; Schmid, R.D. CYP175A1 from *Thermus thermophilus* HB27, the first beta-carotene hydroxylase of the P450 superfamily. *Appl. Microbiol. Biotechnol.* **2004**, *64*, 671–674. [[CrossRef](#)]
14. Yano, J.K.; Blasco, F.; Li, H.; Schmid, R.D.; Henne, A.; Poulos, T.L. Preliminary characterization and crystal structure of a thermostable cytochrome P450 from *Thermus thermophilus*. *J. Biol. Chem.* **2003**, *278*, 608–616. [[CrossRef](#)]
15. Harris, K.L.; Thomson, R.E.S.; Strohmaier, S.J.; Gumulya, Y.; Gillam, E.M.J. Determinants of thermostability in the cytochrome P450 fold. *Biochim. Biophys. Acta Proteins Proteom.* **2018**, *1866*, 97–115. [[CrossRef](#)] [[PubMed](#)]
16. Tavanti, M.; Porter, J.L.; Sabatini, S.; Turner, N.J.; Flitsch, S.L. Panel of New Thermostable CYP116B Self-Sufficient Cytochrome P450 Monooxygenases that Catalyze C–H Activation with a Diverse Substrate Scope. *ChemCatChem* **2018**, *10*, 1042–1051. [[CrossRef](#)]
17. Gumulya, Y.; Baek, J.-M.; Wun, S.-J.; Thomson, R.E.S.; Harris, K.L.; Hunter, D.J.B.; Behrendorff, J.B.Y.H.; Kulig, J.; Zheng, S.; Wu, X.; et al. Engineering highly functional thermostable proteins using ancestral sequence reconstruction. *Nat. Catal.* **2018**, *1*, 878–888. [[CrossRef](#)]
18. Kubota, M.; Nodate, M.; Yasumoto-Hirose, M.; Uchiyama, T.; Kagami, O.; Shizuri, Y.; Misawa, N. Isolation and functional analysis of cytochrome P450 CYP153A genes from various environments. *Biosci. Biotechnol. Biochem.* **2005**, *69*, 2421–2430. [[CrossRef](#)]
19. Kim, B.S.; Kim, S.Y.; Park, J.; Park, W.; Hwang, K.Y.; Yoon, Y.J.; Oh, W.K.; Kim, B.Y.; Ahn, J.S. Sequence-based screening for self-sufficient P450 monooxygenase from a metagenome library. *J. Appl. Microbiol.* **2007**, *102*, 1392–1400. [[CrossRef](#)] [[PubMed](#)]
20. López-López, O.; Cerdán, M.E.; González-Siso, M.I. Hot spring metagenomics. *Life* **2013**, *3*, 308–320. [[CrossRef](#)]
21. Tung, N.V.; Hoang, N.H.; Thoa, N.K. Mining cytochrome p450 genes through next generation sequencing and metagenomic analysis from Binh Chau hot spring. *Acad. J. Biol.* **2019**, *41*. [[CrossRef](#)]
22. Kelly, D.E.; Kraševac, N.; Mullins, J.; Nelson, D.R. The CYPome (Cytochrome P450 complement) of *Aspergillus nidulans*. *Fungal Genet. Biol.* **2009**, *46*, S53–S61. [[CrossRef](#)] [[PubMed](#)]
23. Martinis, S.A.; Atkins, W.M.; Stayton, P.S.; Sligar, S.G. A conserved residue of cytochrome P-450 is involved in heme-oxygen stability and activation. *J. Am. Chem. Soc.* **1989**, *111*, 9252–9253. [[CrossRef](#)]
24. Hasemann, C.A.; Kurumbail, R.G.; Boddupalli, S.S.; Peterson, J.A.; Deisenhofer, J. Structure and function of cytochromes P450: A comparative analysis of three crystal structures. *Structure* **1995**, *3*, 41–62. [[CrossRef](#)]

25. Syed, K.; Mashele, S.S. Comparative analysis of P450 signature motifs EXXR and CXG in the Large and diverse kingdom of fungi: Identification of evolutionarily conserved amino acid patterns characteristic of P450 family. *PLoS ONE* **2014**, *9*, e95616. [[CrossRef](#)]
26. Omura, T.; Sato, R. The carbon monoxide-binding pigment of liver microsomes. I. Evidence for its hemoprotein nature. *J. Biol. Chem.* **1964**, *239*, 2370–2378.
27. Ravichandran, K.G.; Boddupalli, S.S.; Hasermann, C.A.; Peterson, J.A.; Deisenhofer, J. Crystal structure of hemoprotein domain of P450BM-3, a prototype for microsomal P450's. *Science* **1993**, *261*, 731–736. [[CrossRef](#)]
28. Luthra, A.; Denisov, I.G.; Sligar, S.G. Spectroscopic features of cytochrome P450 reaction intermediates. *Arch. Biochem. Biophys.* **2011**, *507*, 26–35. [[CrossRef](#)]
29. Mak, P.J.; Denisov, I.G. Spectroscopic studies of the cytochrome P450 reaction mechanisms. *Biochim. Biophys. Acta* **2018**, *1866*, 178–204. [[CrossRef](#)]
30. Greenfield, N.J. Using circular dichroism spectra to estimate protein secondary structure. *Nat. Protoc.* **2006**, *1*, 2876–2890. [[CrossRef](#)]
31. Milhim, M.; Gerber, A.; Neunzig, J.; Hannemann, F.; Bernhardt, R. A Novel NADPH-dependent flavoprotein reductase from *Bacillus megaterium* acts as an efficient cytochrome P450 reductase. *J. Biotechnol.* **2016**, *231*, 83–94. [[CrossRef](#)]
32. Milhim, M.; Putkaradze, N.; Abdulmughni, A.; Kern, F.; Hartz, P.; Bernhardt, R. Identification of a new plasmid-encoded cytochrome P450 CYP107DY1 from *Bacillus megaterium* with a catalytic activity towards mevastatin. *J. Biotechnol.* **2016**, *240*, 68–75. [[CrossRef](#)] [[PubMed](#)]
33. Müller, J.J.; Hannemann, F.; Schiffler, B.; Ewen, K.M.; Kappl, R.; Heinemann, U.; Bernhardt, R. Structural and thermodynamic characterization of the adrenodoxin-like domain of the electron-transfer protein Etp1 from *Schizosaccharomyces pombe*. *J. Inorg. Biochem.* **2011**, *105*, 957–965. [[CrossRef](#)] [[PubMed](#)]
34. Kleser, M.; Hannemann, F.; Hutter, M.; Zapp, J.; Bernhardt, R. CYP105A1 mediated 3-hydroxylation of glimepiride and glibenclamide using a recombinant *Bacillus megaterium* whole-cell catalyst. *J. Biotechnol.* **2012**, *157*, 405–412. [[CrossRef](#)] [[PubMed](#)]
35. Janocha, S.; Bernhardt, R. Design and characterization of an efficient CYP105A1-based whole-cell biocatalyst for the conversion of resin acid diterpenoids in permeabilized *Escherichia coli*. *Appl. Microbiol. Biotechnol.* **2013**, *97*, 7639–7649. [[CrossRef](#)]
36. Ringle, M.; Khatri, Y.; Zapp, J.; Hannemann, F.; Bernhardt, R. Application of a new versatile electron transfer system for cytochrome P450-based *Escherichia coli* whole-cell bioconversions. *Appl. Microbiol. Biotechnol.* **2013**, *97*, 7741–7754. [[CrossRef](#)]
37. Kern, F.; Khatri, Y.; Litzenburger, M.; Bernhardt, R. CYP267A1 and CYP267B1 from *Sorangium cellulosum* So ce56 are highly versatile drug metabolizers. *Drug Metab. Dispos.* **2016**, *44*, 495–504. [[CrossRef](#)]
38. Khatri, Y.; Hannemann, F.; Girhard, M.; Kappl, R.; Mème, A.; Ringle, M.; Janocha, S.; Leize-Wagner, E.; Urlacher, V.B.; Bernhardt, R. Novel family members of CYP109 from *Sorangium cellulosum* So ce56 exhibit characteristic biochemical and biophysical properties. *Biotechnol. Appl. Biochem.* **2013**, *60*, 18–29. [[CrossRef](#)]
39. Abdulmughni, A.; Jóźwik, I.K.; Brill, E.; Hannemann, F.; Thunnissen, A.-M.W.H.; Bernhardt, R. Biochemical and structural characterization of CYP109A2, a vitamin D3 25-hydroxylase from *Bacillus megaterium*. *FEBS J.* **2017**, *284*, 3881–3894. [[CrossRef](#)]
40. Khatri, Y.; Girhard, M.; Romankiewicz, A.; Ringle, M.; Hannemann, F.; Urlacher, V.B.; Hutter, M.C.; Bernhardt, R. Regioselective hydroxylation of norisoprenoids by CYP109D1 from *Sorangium cellulosum* So ce56. *Appl. Microbiol. Biotechnol.* **2010**, *88*, 485–495. [[CrossRef](#)]
41. Jóźwik, I.K.; Kiss, F.M.; Gricman, Ł.; Abdulmughni, A.; Brill, E.; Zapp, J.; Pleiss, J.; Bernhardt, R.; Thunnissen, A.-M.W.H. Structural basis of steroid binding and oxidation by the cytochrome P450 CYP109E1 from *Bacillus megaterium*. *FEBS J.* **2016**, *283*, 4128–4148. [[CrossRef](#)] [[PubMed](#)]
42. Girhard, M.; Klaus, T.; Khatri, Y.; Bernhardt, R.; Urlacher, V.B. Characterization of the versatile monooxygenase CYP109B1 from *Bacillus subtilis*. *Appl. Microbiol. Biotechnol.* **2010**, *87*, 595–607. [[CrossRef](#)] [[PubMed](#)]
43. Zhang, A.; Zhang, T.; Hall, E.A.; Hutchinson, S.; Cryle, M.J.; Wong, L.-L.; Zhou, W.; Bell, S.G. The crystal structure of the versatile cytochrome P450 enzyme CYP109B1 from *Bacillus subtilis*. *Mol. Biosyst.* **2015**, *11*, 869–881. [[CrossRef](#)] [[PubMed](#)]
44. Putkaradze, N.; Litzenburger, M.; Abdulmughni, A.; Milhim, M.; Brill, E.; Hannemann, F.; Bernhardt, R. CYP109E1 is a novel versatile statin and terpene oxidase from *Bacillus megaterium*. *Appl. Microbiol. Biotechnol.* **2017**, *101*, 8379–8393. [[CrossRef](#)] [[PubMed](#)]

45. Putkaradze, N.; Litzenburger, M.; Hutter, M.C.; Bernhardt, R. CYP109E1 from *Bacillus megaterium* acts as a 24- and 25-Hydroxylase for cholesterol. *ChemBioChem* **2019**, *20*, 655–658. [[CrossRef](#)]
46. Park, S.-Y.; Yamane, K.; Adachi, S.; Shiro, Y.; Weiss, K.E.; Maves, S.A.; Sligar, S.G. Thermophilic cytochrome P450 (CYP119) from *Sulfolobus solfataricus*: High resolution structure and functional properties. *J. Inorg. Biochem.* **2002**, *91*, 491–501. [[CrossRef](#)]
47. Matsumura, H.; Matsuda, K.; Nakamura, N.; Ohtaki, A.; Yoshida, H.; Kamitori, S.; Yohda, M.; Ohno, H. Monooxygenation by a thermophilic cytochrome P450 via direct electron donation from NADH. *Metallomics* **2011**, *3*, 389–395. [[CrossRef](#)]
48. Schallmeyer, A.; den Besten, G.; Teune, I.G.P.; Kembaren, R.F.; Janssen, D.B. Characterization of cytochrome P450 monooxygenase CYP154H1 from the thermophilic soil bacterium *Thermobifida fusca*. *Appl. Microbiol. Biotechnol.* **2011**, *89*, 1475–1485. [[CrossRef](#)]
49. Ho, W.W.; Li, H.; Nishida, C.R.; Ortiz de Montellano, P.R.; Poulos, T.L. Crystal structure and properties of CYP231A2 from the Thermoacidophilic archaeon *Picrophilus torridus*. *Biochemistry* **2008**, *47*, 2071–2079. [[CrossRef](#)]
50. Li, Z.; Jiang, Y.; Guengerich, F.P.; Ma, L.; Li, S.; Zhang, W. Engineering cytochrome P450 enzyme systems for biomedical and biotechnological applications. *J. Biol. Chem.* **2020**, *295*, 833–849. [[CrossRef](#)]
51. Handelsman, J. Metagenomics: Application of genomics to uncultured microorganisms. *Microbiol. Mol. Biol. Rev.* **2004**, *68*, 669–685. [[CrossRef](#)] [[PubMed](#)]
52. Yang, C.; Xia, Y.; Qu, H.; Li, A.-D.; Liu, R.; Wang, Y.; Zhang, T. Discovery of new cellulases from the metagenome by a metagenomics-guided strategy. *Biotechnol. Biofuels* **2016**, *9*. [[CrossRef](#)] [[PubMed](#)]
53. Henne, A.; Schmitz, R.A.; Bömeke, M.; Gottschalk, G.; Daniel, R. Screening of Environmental dna libraries for the presence of genes conferring lipolytic activity on *Escherichia coli*. *Appl. Environ. Microbiol.* **2000**, *66*, 3113–3116. [[CrossRef](#)] [[PubMed](#)]
54. Wang, Q.; Wu, H.; Wang, A.; Du, P.; Pei, X.; Li, H.; Yin, X.; Huang, L.; Xiong, X. Prospecting metagenomic enzyme subfamily genes for dna family shuffling by a novel pcr-based approach. *J. Biol. Chem.* **2010**, *285*, 41509–41516. [[CrossRef](#)]
55. Yun, J.; Kang, S.; Park, S.; Yoon, H.; Kim, M.-J.; Heu, S.; Ryu, S. Characterization of a novel amylolytic enzyme encoded by a gene from a soil-derived metagenomic library. *Appl. Environ. Microbiol.* **2004**, *70*, 7229–7235. [[CrossRef](#)]
56. Uchiyama, T.; Miyazaki, K. Product-induced gene expression, a product-responsive reporter assay used to screen metagenomic libraries for enzyme-encoding genes. *Appl. Environ. Microbiol.* **2010**, *76*, 7029–7035. [[CrossRef](#)]
57. Knietzsch, A.; Waschkowitz, T.; Bowien, S.; Henne, A.; Daniel, R. Construction and screening of metagenomic libraries derived from enrichment cultures: Generation of a Gene Bank for genes conferring alcohol oxidoreductase activity on *Escherichia coli*. *Appl. Environ. Microbiol.* **2003**, *69*, 1408–1416. [[CrossRef](#)]
58. Knietzsch, A.; Bowien, S.; Whited, G.; Gottschalk, G.; Daniel, R. Identification and characterization of coenzyme B12-dependent glycerol dehydratase- and diol dehydratase-encoding genes from metagenomic DNA libraries derived from enrichment cultures. *Appl. Environ. Microbiol.* **2003**, *69*, 3048–3060. [[CrossRef](#)]
59. Musumeci, M.A.; Lozada, M.; Rial, D.V.; Mac Cormack, W.P.; Jansson, J.K.; Sjöling, S.; Carroll, J.; Dionisi, H.M. Prospecting biotechnologically-relevant monooxygenases from cold sediment metagenomes: An in silico approach. *Mar. Drugs* **2017**, *15*, 114. [[CrossRef](#)]
60. Gabor, E.M.; Alkema, W.B.L.; Janssen, D.B. Quantifying the accessibility of the metagenome by random expression cloning techniques. *Environ. Microbiol.* **2004**, *6*, 879–886. [[CrossRef](#)]
61. Tirawongsaroj, P.; Sriprang, R.; Harnpicharnchai, P.; Thongaram, T.; Champreda, V.; Tanapongpipat, S.; Pootanakit, K.; Eurwilaichitr, L. Novel thermophilic and thermostable lipolytic enzymes from a Thailand hot spring metagenomic library. *J. Biotechnol.* **2008**, *133*, 42–49. [[CrossRef](#)]
62. Sharma, P.K.; Singh, K.; Singh, R.; Capalash, N.; Ali, A.; Mohammad, O.; Kaur, J. Characterization of a thermostable lipase showing loss of secondary structure at ambient temperature. *Mol. Biol. Rep.* **2012**, *39*, 2795–2804. [[CrossRef](#)] [[PubMed](#)]
63. Zhou, X.-X.; Wang, Y.-B.; Pan, Y.-J.; Li, W.-F. Differences in amino acids composition and coupling patterns between mesophilic and thermophilic proteins. *Amino Acids.* **2008**, *34*, 25–33. [[CrossRef](#)]
64. Lee, C.-W.; Wang, H.-J.; Hwang, J.-K.; Tseng, C.-P. Protein thermal stability enhancement by designing salt bridges: A combined computational and experimental study. *PLoS ONE* **2014**, *9*. [[CrossRef](#)]

65. Argos, P.; Rossmann, M.G.; Grau, U.M.; Zuber, H.; Frank, G.; Tratschin, J.D. Thermal stability and protein structure. *Biochemistry* **1979**, *18*, 5698–5703. [[CrossRef](#)] [[PubMed](#)]
66. Kumar, S.; Tsai, C.J.; Nussinov, R. Factors enhancing protein thermostability. *Protein Eng.* **2000**, *13*, 179–191. [[CrossRef](#)] [[PubMed](#)]
67. Pack, S.P.; Yoo, Y.J. Packing-based difference of structural features between thermophilic and mesophilic proteins. *Int. J. Biol. Macromol.* **2005**, *35*, 169–174. [[CrossRef](#)] [[PubMed](#)]
68. Saab-Rincón, G.; Alwaseem, H.; Guzmán-Luna, V.; Olvera, L.; Fasan, R. Stabilization of the reductase domain in the catalytically self-sufficient cytochrome P450BM3 by consensus-guided mutagenesis. *ChemBioChem* **2018**, *19*, 622–632. [[CrossRef](#)]
69. Eiben, S.; Bartelmäs, H.; Urlacher, V.B. Construction of a thermostable cytochrome P450 chimera derived from self-sufficient mesophilic parents. *Appl. Microbiol. Biotechnol.* **2007**, *75*, 1055–1061. [[CrossRef](#)]
70. Goyal, S.; Banerjee, S.; Mazumdar, S. Oxygenation of monoenoic fatty acids by CYP175A1, an orphan cytochrome P450 from *Thermus thermophilus* HB27. *Biochemistry* **2012**, *51*, 7880–7890. [[CrossRef](#)]
71. Salamanca-Pinzon, S.G.; Khatri, Y.; Carius, Y.; Keller, L.; Müller, R.; Lancaster, C.R.D.; Bernhardt, R. Structure-function analysis for the hydroxylation of  $\Delta^4$  C21-steroids by the myxobacterial CYP260B1. *FEBS Lett.* **2016**, *590*, 1838–1851. [[CrossRef](#)] [[PubMed](#)]
72. Sheng, Z.; Ge, S.; Gao, M.; Jian, R.; Chen, X.; Xu, X.; Li, D.; Zhang, K.; Chen, W.-H. Synthesis and biological activity of embelin and its derivatives: An overview. *Mini Rev. Med. Chem.* **2020**, *20*, 396–407. [[CrossRef](#)] [[PubMed](#)]
73. Jones, H.; Blanc, D.; Cunliffe, W.J. 13-cis retinoic acid and acne. *Lancet* **1980**, *316*, 1048–1049. [[CrossRef](#)]
74. Schroeder, M.; Zouboulis, C.C. All-trans-retinoic acid and 13-cis-retinoic acid: Pharmacokinetics and biological activity in different cell culture models of human keratinocytes. *Horm. Metab. Res.* **2007**, *39*, 136–140. [[CrossRef](#)]
75. Zasada, M.; Budzisz, E. Retinoids: Active molecules influencing skin structure formation in cosmetic and dermatological treatments. *Postepy Dermatol. Alergol.* **2019**, *36*, 392–397. [[CrossRef](#)]
76. Zhang, X.; Peng, Y.; Zhao, J.; Li, Q.; Yu, X.; Acevedo-Rocha, C.G.; Li, A. Bacterial cytochrome P450-catalyzed regio- and stereoselective steroid hydroxylation enabled by directed evolution and rational design. *Bioresour. Bioprocess.* **2020**, *7*, 2. [[CrossRef](#)]
77. Nelson, D.R. The cytochrome p450 homepage. *Hum. Genom.* **2009**, *4*, 59–65. [[CrossRef](#)]
78. Sievers, F.; Wilm, A.; Dineen, D.; Gibson, T.J.; Karplus, K.; Li, W.; Lopez, R.; McWilliam, H.; Remmert, M.; Söding, J.; et al. Fast, scalable generation of high-quality protein multiple sequence alignments using Clustal Omega. *Mol. Syst. Biol.* **2011**, *7*, 539. [[CrossRef](#)]
79. Kumar, S.; Stecher, G.; Li, M.; Nnyaz, C.; Tamura, K. MEGA X: Molecular evolutionary genetics analysis across computing platforms. *Mol. Biol. Evol.* **2018**, *35*, 1547–1549. [[CrossRef](#)]
80. Le, S.Q.; Gascuel, O. An improved general amino acid replacement matrix. *Mol. Biol. Evol.* **2008**, *25*, 1307–1320. [[CrossRef](#)]
81. Jones, D.T. Protein secondary structure prediction based on position-specific scoring matrices. *J. Mol. Biol.* **1999**, *292*, 195–202. [[CrossRef](#)] [[PubMed](#)]
82. Zhang, X.-F.; Yang, G.-Y.; Zhang, Y.; Xie, Y.; Withers, S.G.; Feng, Y. A general and efficient strategy for generating the stable enzymes. *Sci. Rep.* **2016**, *6*, 33797. [[CrossRef](#)] [[PubMed](#)]
83. Singh, A.K.; Chhatpar, H.S. Purification, characterization and thermodynamics of antifungal protease from *Streptomyces* sp. A6. *J. Basic Microbiol.* **2011**, *51*, 424–432. [[CrossRef](#)] [[PubMed](#)]

